Hindawi
Wireless Communications and Mobile Computing
Volume 2021, Article ID 9966581, 18 pages
https://doi.org/10.1155/2021/9966581

Research Article

Muli-UWB Antenna System Design for 5G Wireless Applications with Diversity

Marwa Daghari[1], **Chaker Essid**[2] and **Hedi Sakli**[1]

[1]*MACS Research Laboratory, National Engineering School of Gabes (ENIG), Gabes University, 6029, LR16ES22, Tunisia*
[2]*SERCOM Laboratory, Tunisia Polytechnic School, University of Carthage, Box 743-2078 La Marsa, Tunisia*

Correspondence should be addressed to Marwa Daghari; marwadaghari@gmail.com

Received 9 March 2021; Accepted 19 May 2021; Published 9 June 2021

Academic Editor: Kasturi Vasudevan

In this paper, we propose a compact Multiple Input Multiple Output (MIMO) antenna system with high isolation for wireless applications in 5G connected devices. This MIMO antenna system with the size of $92 \times 88\,mm^2$ consists of two elliptical antennas symmetrically arranged next to each other. Two decoupling methods which are neutralization and Defected Ground Structure (DGS) are applied to ensure diversity of the proposed MIMO antenna. The single and MIMO antennas are simulated and analyzed then fabricated and measured. A good agreement between measurements and simulations is obtained. These configurations, dedicated to covering the 3.4 GHz band -3.8 GHz, have shown very satisfactory performances more than -30 dB in terms of reduction of mutual coupling between the antennas constituting our system. MIMO diversity parameters, such as Envelope Correlation (ECC), Diversity Gain (DG), and total efficiency, are also studied for each proposed MIMO system. Thus, results demonstrate that our two proposed antenna configurations are very suitable for 5G MIMO applications.

1. Introduction

Wireless communication has become one of the fastest-growing and dynamic technologies around the world over the past two decades. It is widely distributed in our home space and finds many applications in electronic products used in our daily life such as televisions, cell phones, and computers [1]. With the advent of the fifth-generation (5G), we are talking about "all connected" or Internet of Things (IOT) [2]. These are electronic wireless connected devices, sharing information with a computer, tablet, or smartphone and able to perceive, analyze, and act according to the contexts of the environment in which they are located [3].

This rapid advancement in modern wireless technology and especially with 5G allows a large number of new features such as increased data rate and high-quality transmission speed [4].

One of the most important elements of a wireless communication subsystem is the antenna, which is used for the transmission and reception of signals in one direction, and with a specific strength [5]. Depending on the application, there are different challenges in the antenna design. In this context and in order to increase the transmission rate without increasing the power of the transmitted signal or the bandwidth, one solution is to take advantage of the diversity by using several antennas at the same time in transmission and reception [6]. This is the MIMO technique (Multiple Inputs Multiple Outputs). This technique is well known as one of the basic technologies of 5G communication [7]. In fact, it consists in using several antennas, both on the transmission and reception. Thus, we can obtain a significant gain in capacity compared to the conventional Single Input Single Output (SISO) system [8]. This can then provide a gain of diversity that subsequently improves the capacity and quality of the link in the systems [9]. Therefore, increasing the number of antennas on electronics terminals is an option to increase the capacity of the channel. In this case, the distance of the separation between the different antennas must be sufficient to guarantee the independence of the signals [10].

However, this distance is limited by the space reserved for an antenna in the electronic components [11]. This results into a strong and inevitable mutual coupling between the

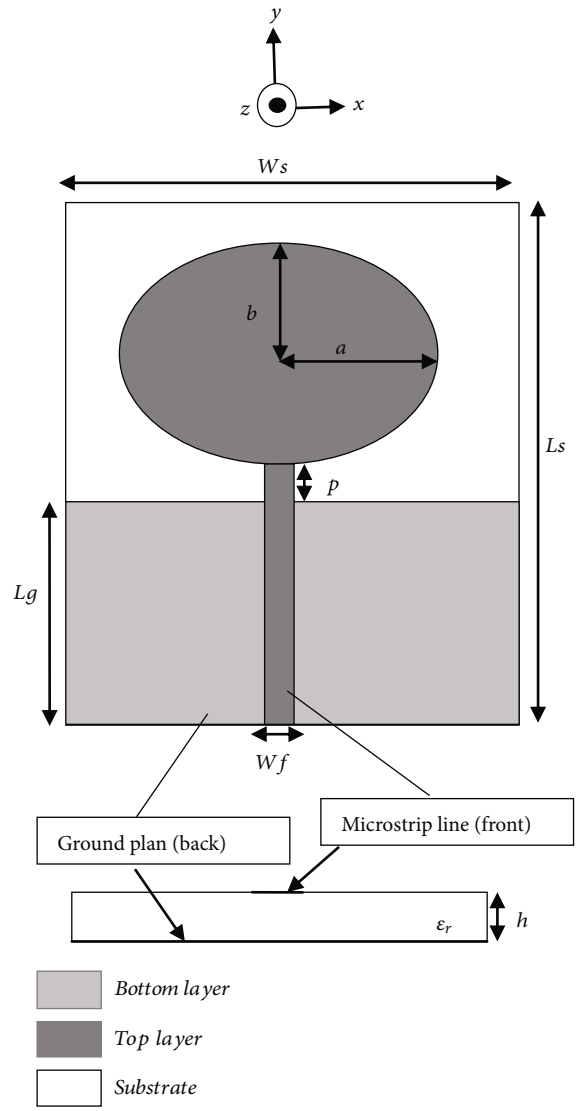

Figure 1: Elliptical antenna geometry.

antenna elements that are closely spaced. Because of this mutual coupling, the effectiveness of the multiantenna system decreases, and performance is affected. However, reducing this mutual coupling is not an easy task especially for low frequencies where the currents flowing on the ground plan are not negligible and can contribute to the radiation of the mechanism of the whole structure [12, 13].

In order to overcome this problem of mutual coupling, the isolation between the antennas should be high in the radiator design. Especially with the design of small antennas, achieving high isolation becomes a major challenge. Several methods known as isolation techniques have been studied and used on multiantenna and MIMO systems to reduce this strong coupling [14]. Isolation techniques can ensure the proper functioning of antennas in the multiantenna and/or MIMO systems. In this context, a lot of research has already been done on multiantenna systems in telecommunications. Most of them concern the field of mobile telephony due to the limited size of smartphones and especially their very

Table 1: Temperature and wildlife count in the three areas covered by the study.

Patch dimensions	Ground plan dimensions	Substrate dimensions
$a = 14.5$ mm	$L_g = 19$ mm	$L_s = 44$ mm
$b = 10$ mm	$W_g = 46$ mm	$W_s = 46$ mm
$p = 0.4$ mm		
$W_f = 3$ mm		

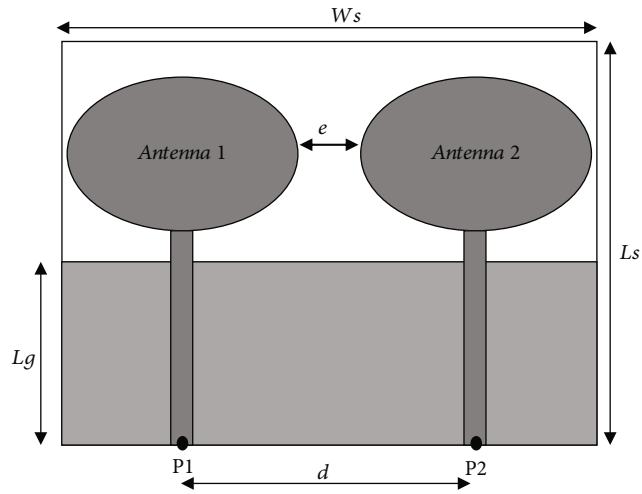

Figure 2: Proposed multiantenna system geometry.

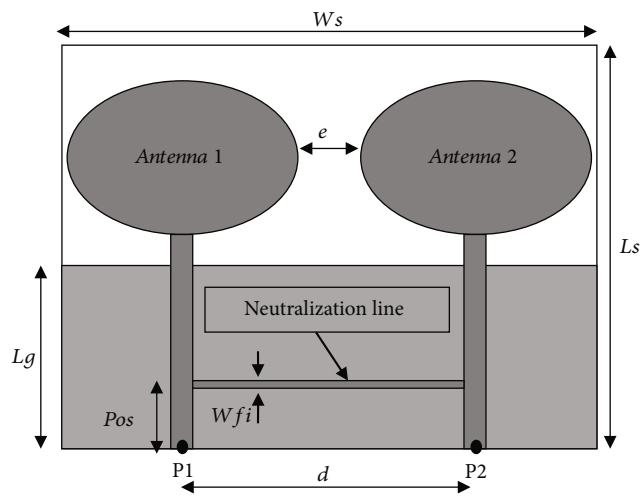

Figure 3: Multiantenna system configuration with neutralization line.

small slots reserved for antennas [15–17]. Few other works concern Ultra Wide Band (UWB) applications [18–21]. The idea developed by these researchers is based on modifying the ground plan and engraving slots in it. These structures are known as Defected Ground Structure (DGS) [22]. In fact, the phenomenon responsible for coupling is the current flowing through the ground plan from one radiating element to another. For this, the isolation is ensured by reducing the flow of currents in this plan through the presence of slots.

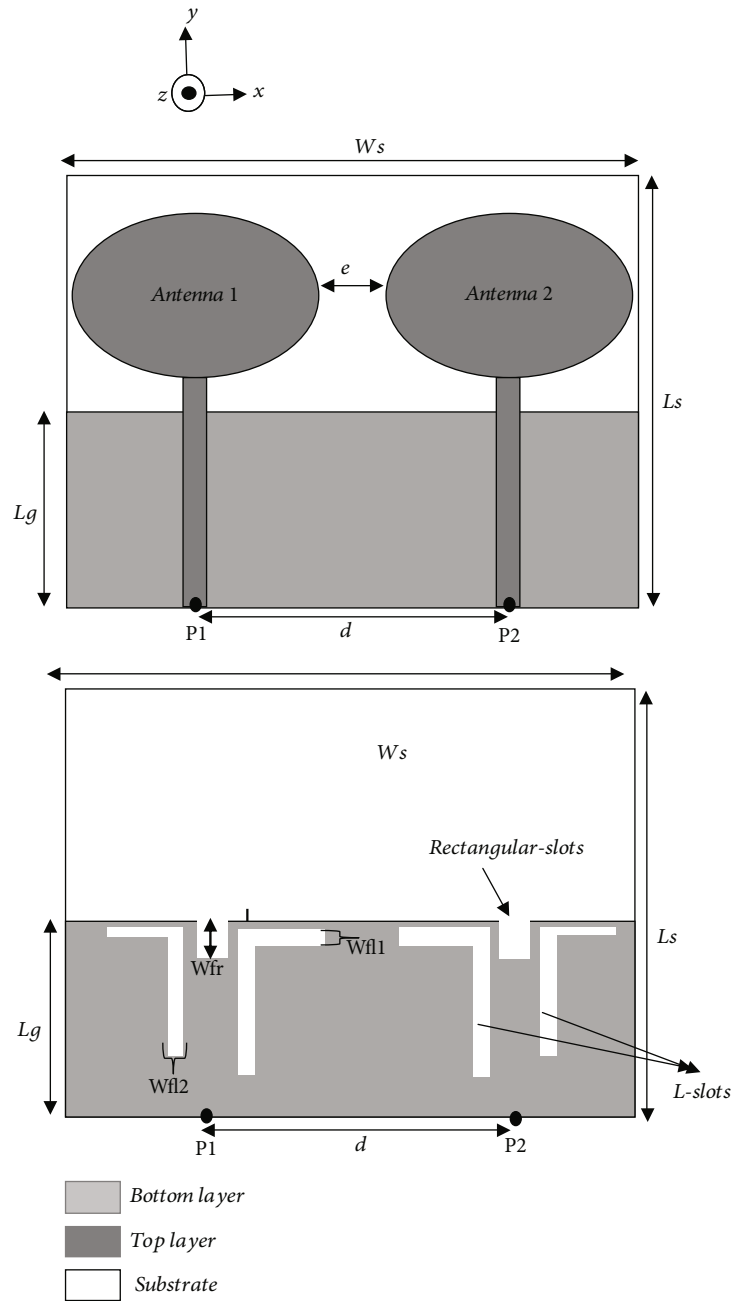

Figure 4: Multiantenna MIMO system structure with DGS (on top and bottom view).

In the paper [18], we show that a compact dumbbell-shaped ground structure (DGS) is applied to reduce the mutual coupling between the patch antenna array elements spaced 0.47λ. The DGS dumbbell is inserted between adjacent coupled antennas to suppress pronounced surface waves. Results show a mutual coupling reduction of 20 dB around the resonant frequency of 5.646 GHz. In order to reduce mutual coupling, the authors in [19] add a narrow slot in the ground plane of a ULB MIMO system of two L-shaped slot antennas. The results prove that the proposed antenna shows a bandwidth greater than 3.1-10.6 GHz with a low mutual coupling of less than 15 dB over the entire UWB band. Research in [20] adopts the same technique in the isolation between elements of a patch antenna array. This method provides a coupling of minus -17 dB over the frequency range of 3.1 GHz to 11 GHz, which has resulted in an improvement in the performance of the system by increasing gain, reliability, and connectivity. A compact ULB MIMO antenna has also been proposed in [21]. It consists of two slotted ULB antennas placed in a small space of 22 mm × 26 mm. A T-shaped slot is engraved on the ground plane to improve the impedance matching characteristic in low frequencies and reduce mutual coupling for frequencies above 4 GHz. A line slot is added to cancel the original coupling and provide isolation. Results show a low mutual coupling of less than -18 dB over the operating band from

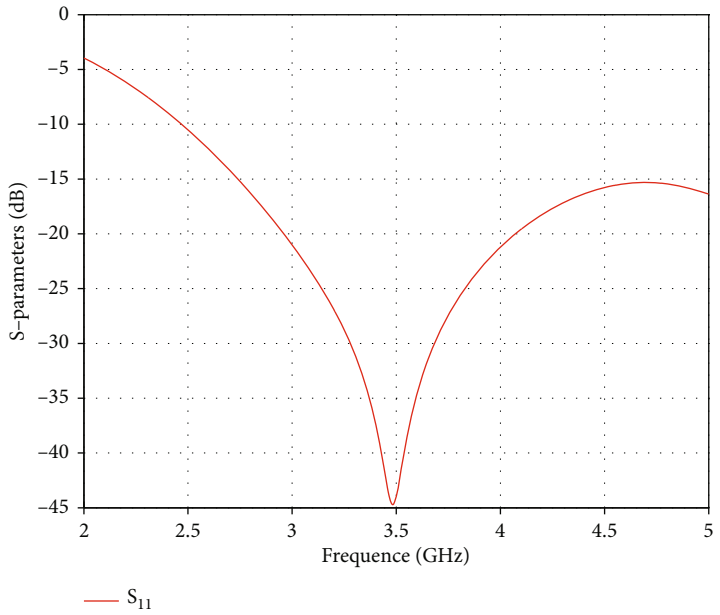

Figure 5: Reflection coefficient S_{11} of the elliptical antenna as a function of frequency.

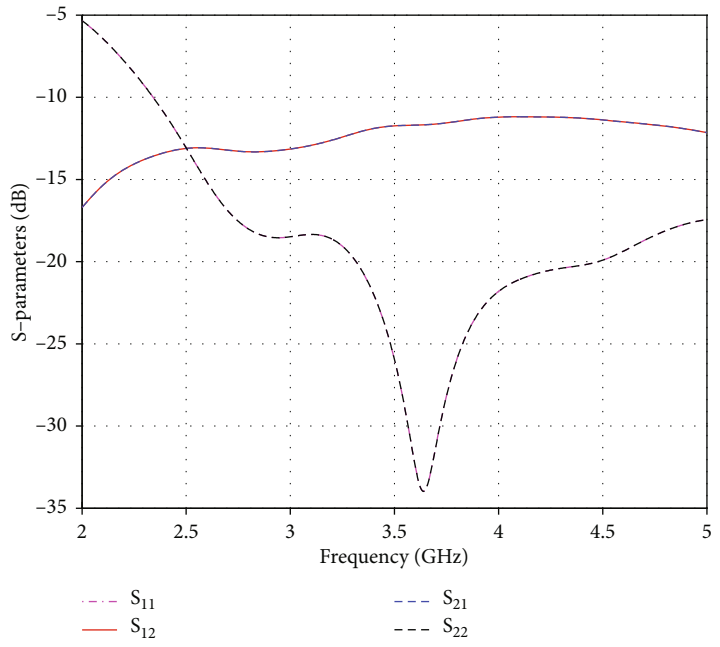

Figure 6: Simulated S-parameters of multiantenna system without isolation.

3.1 to 10.6 GHz. The performance of isolation can overcome the fading problem caused by multipath propagation in various UWB systems.

Another very original decoupling technique often used is called "neutralization technique" [23]. The latter ensures the blocking of the mutual coupling by carefully inserting an inductance, usually modeled as a transmission line, between the radiating elements to obtain a global behavior of a rejector filter. Several other works have confirmed the reliability of this neutralization solution in reducing mutual coupling between the elements of a multiantenna and/or MIMO system in variable application domains [22, 24, 25]. Some of these researches have shown that this technique could work on different types of antennas and other ground plane forms as well as other frequency bands. In fact, in [26], two circular monopoles separated by a distance of 2.2 mm are printed on the FR-4 substrate. A neutralization line is connected and interlaced between the two monopoles on the substrate. This line inserted between the two antennas provides an insolation of more than 22 dB. In the same way, authors in [27], proposed a 4×4 compact MIMO antennas that are designed and tested for very wideband applications. A neutralization

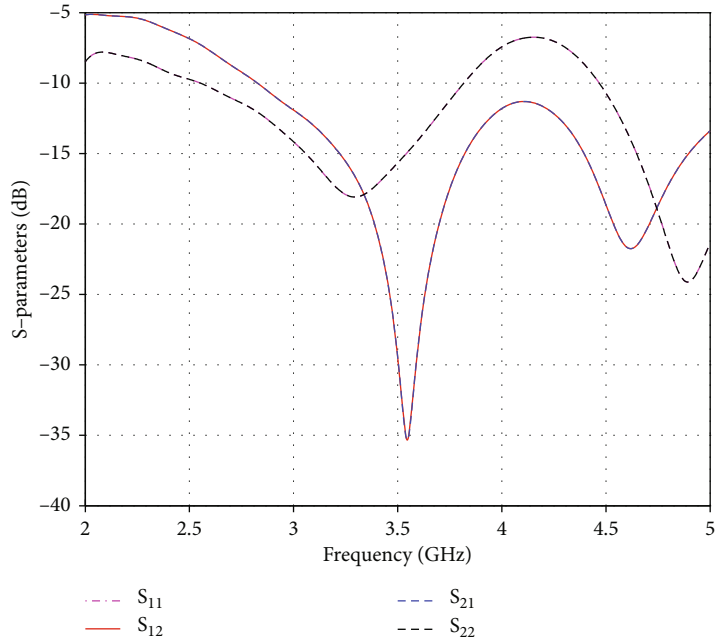

Figure 7: Simulated *S*-parameters of multiantenna system with isolation.

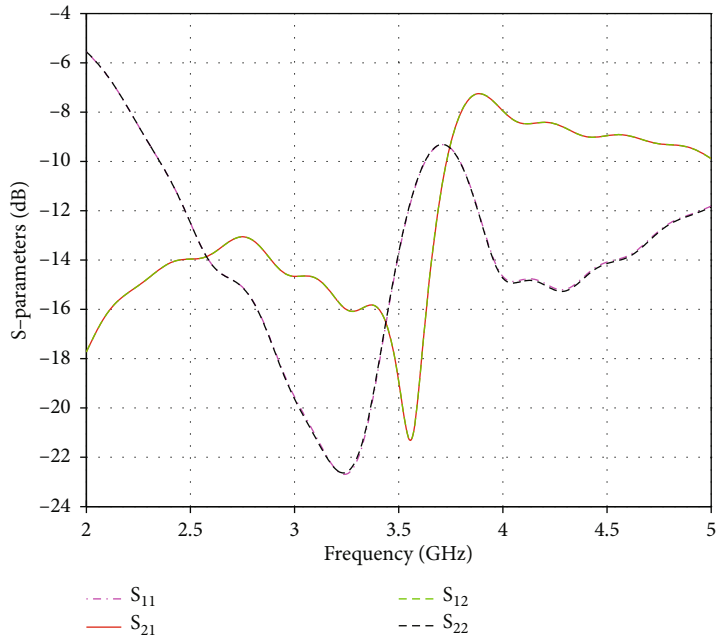

Figure 8: Simulated *S*-parameters of the multiantenna system with DGS.

line is composed of two narrow bands and a rectangular metal band on the center which are directly connected to the closely spaced monopole antennas. By using this technique, the mutual coupling between the radiating elements is greatly reduced to -23 dB, resulting then, in an improvement of the overall system performance in gain, radiation efficiency, and diversity. This technique of isolation with neutralization, which we have already mentioned, is also adopted by the authors in [28]. The multiantenna system is composed by two monopoles slotted in D-shape with a three-branch neutralization line inserted between them. The use of this line reduced the coupling from 5.4 dB to more than 20 dB over the entire 8.90-14.90 GHz frequency band.

In the state of the art presented above, it has been shown that the reduction of coupling with isolation techniques conditions the diversity performance of multiantenna and/or MIMO systems. Therefore, we propose in this paper two multiantenna UWB systems designs with isolation techniques for 5G wireless applications with diversity. These systems consist of two UWB elliptical monopole antennas with

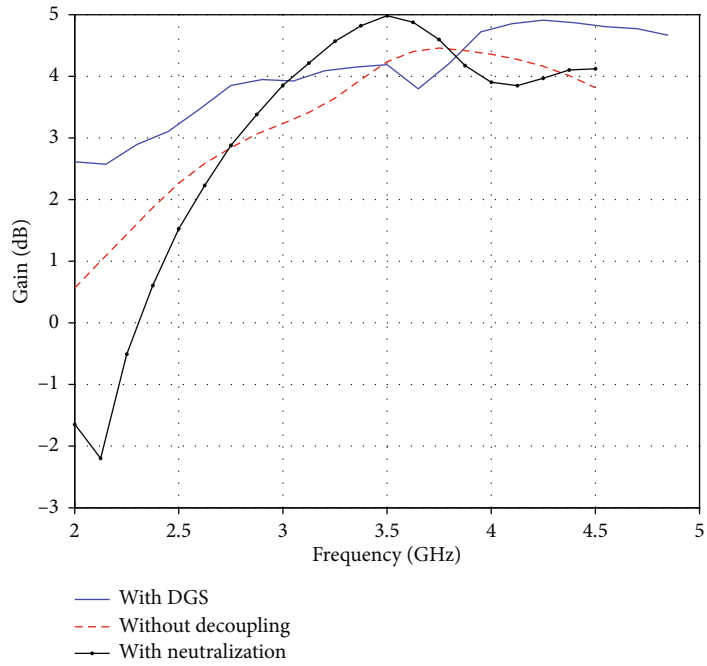

Figure 9: Multiantennas system gain variation with and without decoupling techniques.

high isolation using the neutralization technique for the first, whereas the second is made using defected ground structures to ensure isolation between elliptical antennas. These configurations, dedicated to covering the 3.4-3.8 GHz band, have shown very satisfactory performances in terms of reduction of mutual coupling between the antennas constituting our system. These results have also been validated by prototypes and measurements.

The rest of the paper is based on different sections: Section II describes the proposed multiantennas systems geometries. Then, simulation results of the different antenna systems are detailed in Section III. Measurement works are presented in Section VI. Decoupling performances of the different geometries are discussed in Section V, and conclusions are finally presented in the last section.

2. Multi antenna System Geometry

Obtaining initial target criteria in the design of a multiantenna system ensures the proper functioning and overall performance of the suggested design. In our proposal, we have listed some of the key objectives to be achieved:

(i) *Choice of the Shape of the Antenna Element.* UWB printed antennas have several advantages. Precisely, the monopoles in planar technology represent our choice in this study. In fact, in comparison with the other UWB monopole antennas, the elliptical shape offers the widest bandwidth. In addition, few works in the scientific researchers have used the elliptical form in the design of multiantenna systems. For this reason, we have adopted this choice as the basic shape for the antenna element constituting our proposed multiantenna system

(ii) *Choice of Study Frequency.* As we have chosen the UWB technology, the main band planned is between 3.1 GHz and 10.6 GHz. On the other hand, at the World Radiocommunication Conference (WRC) in 2015, the 3.5 GHz band (3.4 GHz-3.8 GHz) is the band that will be used initially by 5G [13]. More specifically, the 3.5 GHz frequency is used in France by Orange for applications of devices connected in 5G. Consequently, this frequency is our choice in the design of the multiantenna system proposed in this study

(iii) *Choice of Isolation Techniques.* In wireless communications, the development of multiantenna systems is evolving with the emergence of new standards and in particular with 5G. As we have already mentioned in the introduction, isolation techniques represent a powerful solution to design systems in diversity and MIMO especially with the miniaturization of devices. We have chosen two techniques in the design of our multiantenna system. These are the neutralization technique and the Defected Ground Structure (DGS) technique. This choice stems from the simplicity of implementation in the design as well as the realization of these structures

2.1. Proposed Elliptical Antenna Element Design. As the proposed system is a MIMO type with two elements, we first designed the antenna element. As already mentioned previously, the elliptical planar monopole is chosen as the radiating element forming the multiantenna system. In [29, 30], this type is made for different UWB applications. The geometry of the proposed antenna is shown in Figure 1. Indeed, the radiator is a patch elliptical shape with the major axis of

2a, a minor axis of 2b, and excited via a microstrip line of 50 Ω of width Wf. It is printed on a substrate of size $W_s \times L_s$ and thickness hs. The size of the ground plane is chosen rectangular with dimensions $W_g \times L_g$. There is a distance p to set the distance between the radiating element and the ground plan.

The first important step in the design of an antenna is the selection of the substrate. The FR-4 with a thickness of $h = 1.6$ mm of relative permittivity $\varepsilon_r = 4.4$ and of loss tangent $tg\delta = 0.02$ is used in the design of the antenna since it is available in the laboratory. It allows quick and easy manufacturing of prototypes due to its low cost compared to other types of substrates. Referring to equations [31], at 3.5 GHz lower cut-off frequency, the values of the geometrical parameters of the elliptical antenna are estimated and then optimized, and they are listed in Table 1.

2.2. Design of Two-Element Antenna System. We propose in this subsection an antenna system resulting from a juxtaposition of two elliptical antennas which are already studied above. The two antennas of identical size and configuration are placed symmetrically on the same ground plan with their own feed noted port 1 (P1) and port 2 (P2), respectively, of the radiating element 1 and 2. As shown in Figure 2, these antennas are spaced at a distance of $d = 44$ mm (approximately a $\lambda_0/2$ with λ_0 being free-space wavelength at the center frequency 3.5 GHz) separating the two ports P1 and P2. This means a distance of $e = 15$ mm (approximately $\lambda_0/6$) between the two edges of the elliptical patch.

2.3. Two-Element MIMO Configuration with Neutralization Decoupling Technique. In multiantenna and/or MIMO systems, the isolation between the different elements, which constitute it, is one of the important parameters to be taken into consideration because the existence of mutual coupling influences the diversity performance of the antenna systems. As indicated in the requirements specification section, the neutralization isolation technique was adopted to reduce the coupling between elliptical antennas. This technique consists in connecting the radiating elements to better decouple their power ports. Indeed, to maximize the energy radiated by a powered antenna, it is necessary to ensure that all the energy transmitted to it is not lost in the second antenna. It is therefore necessary to minimize the S_{21} which will be taken as the parameter characterizing the decoupling between the two radiating elements. So, this is ensured by inserting a microstrip transmission line which naturally has a very high characteristic impedance and can be considered as an inductance. The behavior of a rejection filter is achieved to reduce mutual coupling. Our proposed configuration is illustrated in Figure 3. As shown in this figure, between the antenna feeds, we introduce a microstrip line with 41 mm of long and 0.3 mm (Wfi) of width at a distance of 3 mm (Pos) from ports P1 and P2.

2.4. Two-Element MIMO Configuration with DGS Decoupling Technique. The second isolation technique applied in our study is the introduction of slots in the ground plane of a multiantenna system (also called Defected Ground Structure: DGS). The originality of this method to decouple

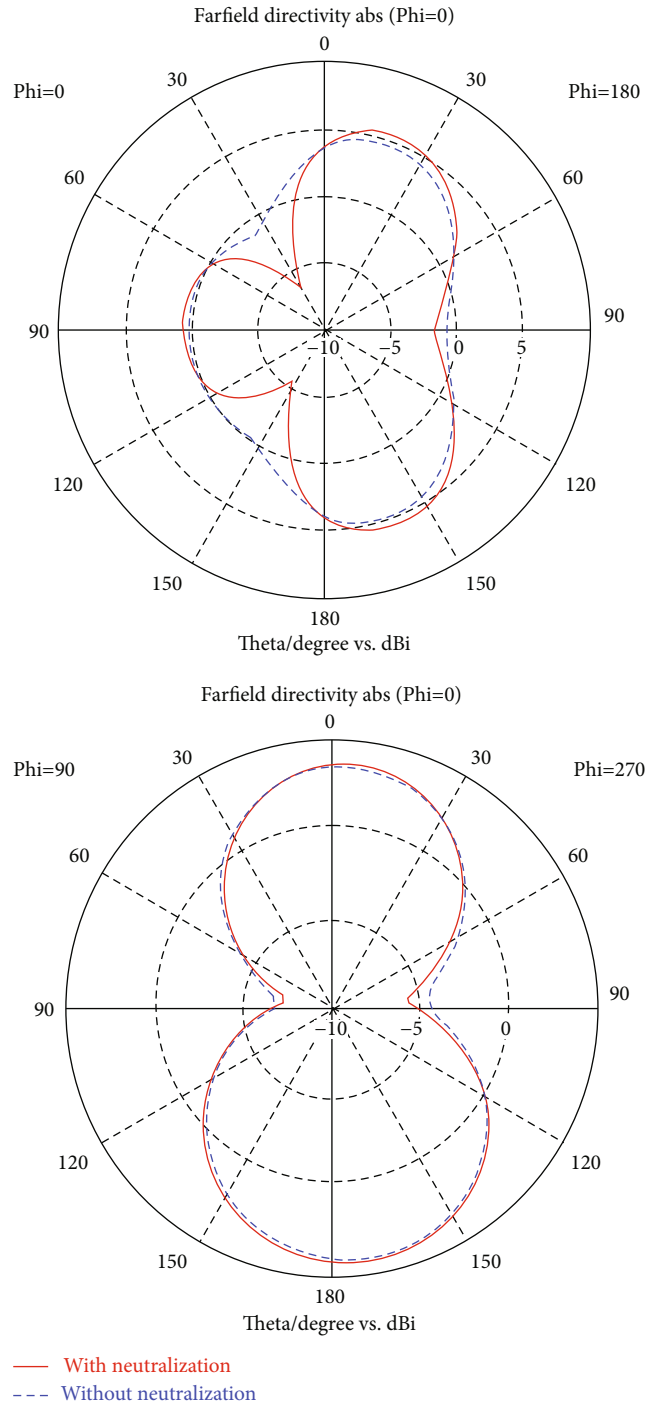

Figure 10: Directivity on 2D of multiantenna systems with and without neutralization for $\varphi = 0°$ and $\varphi = 90°$.

the two ports of the antennas was proved. Indeed, the modification by engraving slots on the ground plan can prevent the propagation of electromagnetic waves. In this case, the coupled fields between the neighboring antennas are eliminated, thanks to the reduction of the current flowing through the ground plan. In order to decouple the two elements of our multiantenna system, we propose to introduce slots in the form of L and others rectangular on the ground plan corresponding to each antenna as shown in Figure 4. Two

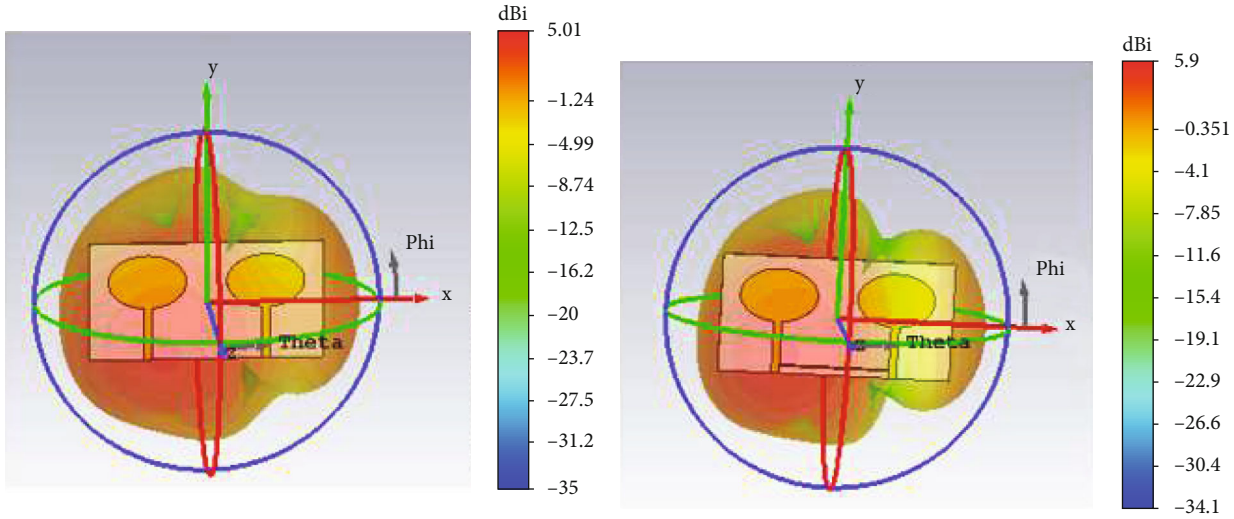

Farfield (f=3.5) (1)

Type	Farfield
Approximation	Enabled (kR>>1)
Component	Abs
Output	Directivity
Frequency	3.5 GHz
Rad. effic	−0.5150 dB
Tot. effic	−0.8278 dB
Dir.	5.007 dBi

(a)

Farfield (f=3.5) (1)

Type	Farfield
Approximation	Enabled (kR>>1)
Component	Abs
Output	Directivity
Frequency	3.5 GHz
Rad. effic	−0.7643 dB
Tot. effic	−0.9169 dB
Dir.	5.899 dBi

(b)

Figure 11: Directivity on 3D of multiantenna systems. (a) Without neutralization. (b) With neutralization.

rectangular slots, each 3 mm (W_{fr}) wide and 2 mm long, are engraved at the top end of the ground plan. The slots L of width 0.7 mm (W_{fl1}) and 0.5 mm (W_{fl2}) are placed on either side of the rectangular slots.

3. Decoupling Simulations Results

3.1. S-Parameters Simulations Results. *S*-parameters describe the input and output relationship between the ports of an electric system. Figure 5 represents the simulated *S*-parameter of the elliptical antenna only. As we can see, a very good adaptation of -43.98 dB is obtained at the 3.5 GHz frequency, which can meet the requirements of 5G wireless applications.

S-parameters simulation results of the proposed multiantenna system without decoupling method are shown in Figure 6. Comparing the simulations of this case with the case where each antenna is alone (Figure 5), we notice that each element resonated at 3.6 GHz with a reflexion coefficient S_{11} value of -46.87 dB. The transmission coefficient S_{21}, which is considered as the parameter characterizing the isolation between the two antenna feed ports, has the value of -11.66 dB at 3.5 GHz. This value of the mutual coupling between the antennas is estimated high. This is due to the insufficient distance between each element, which results in a slight shift of 100 MHz of the resonant from 3.5 GHz to 3.6 GHz.

In Figure 7 below, *S*-parameter simulation results of the proposed multiantenna system with the neutralization decoupling method are presented. In fact, at a frequency of 3.5 GHz, the adaptation of ports P1 and P2 is sufficient ($S_{11} = S_{22} = -16$ dB). On the other hand, a high isolation between P1 and P2 is achieved ($S_{21} = S_{12} < -35$ dB). So, isolation is better with the insertion of a neutralization line.

We illustrate now in Figure 8 the *S*-parameters simulation results of the proposed multiantenna system with DGS configuration. Analyzing this figure, we can remark that at 3.5 GHz study frequency, the adaptation at ports P1 and P2 is sufficient ($S_{11} = S_{22} = -14$ dB). In the other side, a good decoupling between P1 and P2 is achieved ($S_{21} = S_{12} <$ -20 dB). It is clear that the isolation is better with the insertion of slots in the ground plan.

3.2. Radiation Performances Results. In this section, we evaluate the performance of the system with and without isolation techniques in terms of gain, radiation, directivity, and efficiency.

According to Figure 9, the gain did not vary too much and reaches a maximum value at 3.5 GHz frequency for multiantennas systems with decoupling technique (neutralization and DGS). But we note that an increase of 1 dB to reach the 5 dB value in the case of the insertion of the neutralization line. However, it remains stable and reaches a value of 4.3 dB even with a slotted ground plan.

The directivity performances for $\varphi = 0°$ and $\varphi = 90°$ in 2D and 3D of multiantenna systems with and without neutralization isolation techniques are presented in the following Figures 10 and 11. We notice that with the insertion of the neutralization line between the two elliptical antennas, the general radiation pattern characteristics remain constant. Moreover, the directivity is improved from 5.01 dBi to reach

a value of 5.9 dBi. The total efficiency of the antenna system with neutralization is also improved to reach 83% (-0.768 dB). Therefore, with the isolation technique, the system is more directional and more efficient.

The directivity performances for $\varphi = 0^\circ$ and $\varphi = 90^\circ$ in 2D and 3D of multiantenna systems with and without DGS isolation techniques are illustrated in the following Figures 12 and 13. We remark that the efficiency of the antenna system with the DGS isolation technique remains almost constant and equal to 90% (-0.5 dB). However, its directivity is decreased by 0.85 dBi to reach the value of 4.16 dBi. This loss in directivity remains tolerable since the ground plan configuration has been modified.

3.3. Surface Current Distributions. To explain the causes of electromagnetic coupling between very close antennas located on the same ground plan, one approach is to analyze the levels of currents in the ground between them. In this section, the distribution of surface currents at the desired 3.5 GHz frequency for the antenna systems ports will be studied in order to confirm the decoupling between antenna elements. Let us consider that antenna 1 is fed while the second element is switched off. The configuration being symmetrical, we limit ourselves to the study of a single antenna. The visualization of the surface current densities of the antenna structure with and without the neutralization decoupling method is shown in Figure 14. We notice in Figure 14(a) that antenna 2 is radiating but is not fed. This can be explained by the magnetic fields resulting from the circulation of currents in the ground plan which can be assembled. So, a strong electromagnetic coupling is observed. Considering now Figure 14(b) where a neutralization technique was applied, in this case, when antenna 1 is only excited, we observe that there is less current in antenna 2 because all the current is concentrated on the neutralization line. So, the isolation in this case is improved.

We represent in Figure 15 the distribution of the surface current of a multiantenna system with and without DGS. It is clear from Figure 15(b) that when antenna 1 is only excited, a very small value of the current (-28 dB) is recorded on antenna 2. Indeed, the current is concentrated in slots that prevent its circulation to the antenna 2. A strong decoupling in this case is obtained.

4. Fabrication and Measurement Results

4.1. Fabricated Antenna. In order to validate the performances of the elliptical antenna element studied previously, a fabricated prototype is made and it is illustrated in Figure 16. Then, the measurement of the *S*-parameters is carried out using a spectrum analyzer (10 MHz-25 GHz). Simulated and measured S_{11} is shown in Figure 17. Note that the threshold classically used to judge the adaptation is -10 dB, so we conclude on the basis of these results that the curves obtained are quite concordant with an almost similar level and shape. However, a resonance frequency shift of 300 MHz is observed. We believe that this difference is due to the precision of manufacture. Nevertheless, the measurements are in line with our objectives since the module of the S_{11} is less than -20 dB on the working band.

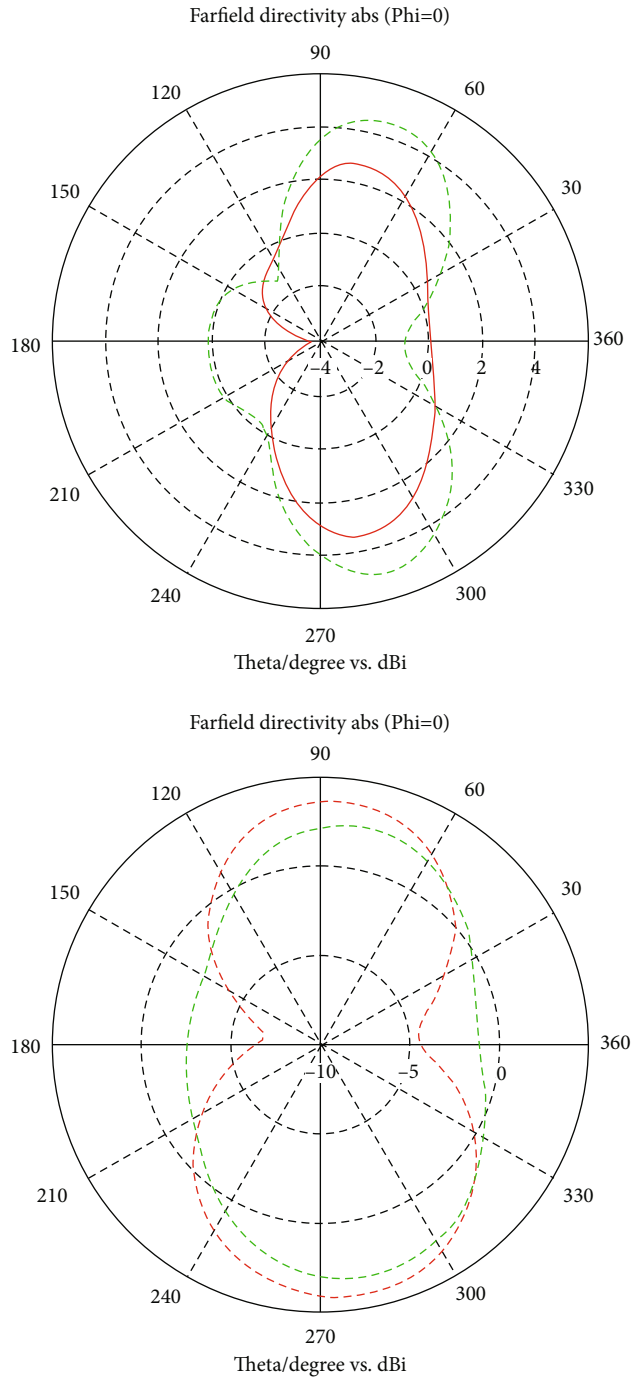

Figure 12: Directivity on 2D of multiantenna systems with and without DGS for $\varphi = 0^\circ$ and $\varphi = 90^\circ$.

4.2. Fabricated Multi antennas Systems with and without Decoupling Technique

4.2.1. Fabricated Multi antennas Systems without Decoupling Technique. Fabricated prototype of the proposed multiantennas system without decoupling technique is made and illustrated in Figure 18. Measurement of the *S*-parameters is

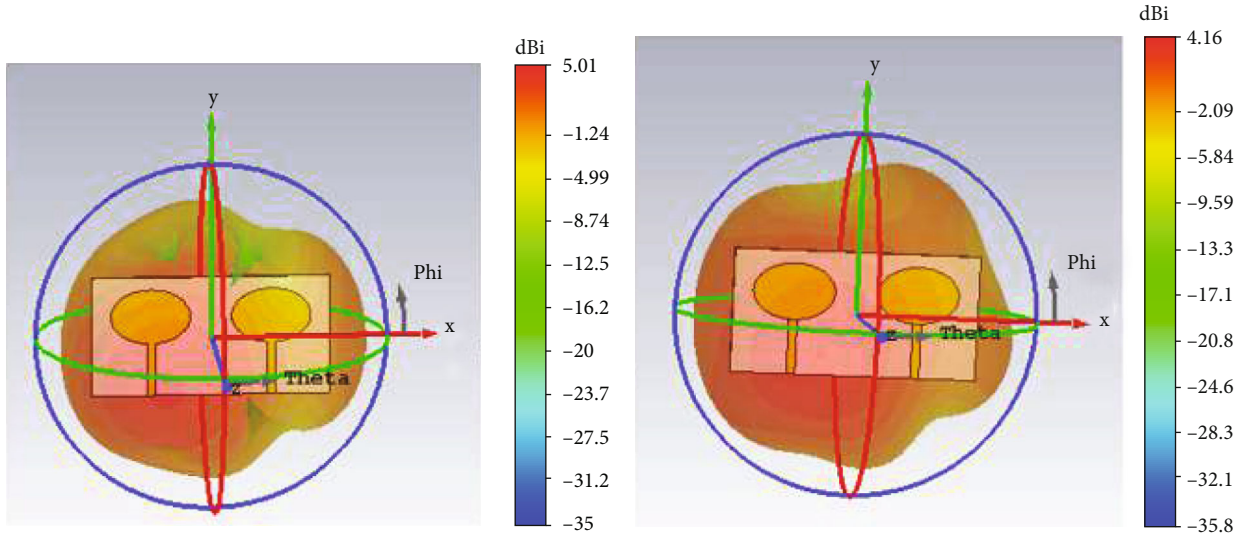

Farfield (f=3.5) (1)

Type	Farfield
Approximation	Enabled (kR>>1)
Component	Abs
Output	Directivity
Frequency	3.5 GHz
Rad. effic	−0.5150 dB
Tot. effic	−0.8278 dB
Dir.	5.007 dBi

(a)

Farfield (f=3.5) (1)

Type	Farfield
Approximation	Enabled (kR>>1)
Component	Abs
Output	Directivity
Frequency	3.5 GHz
Rad. effic	−0.5669 dB
Tot. effic	−0.8068 dB
Dir.	4.158 dBi

(b)

Figure 13: Directivity on 3D of multiantenna systems. (a) Without DGS. (b) With DGS.

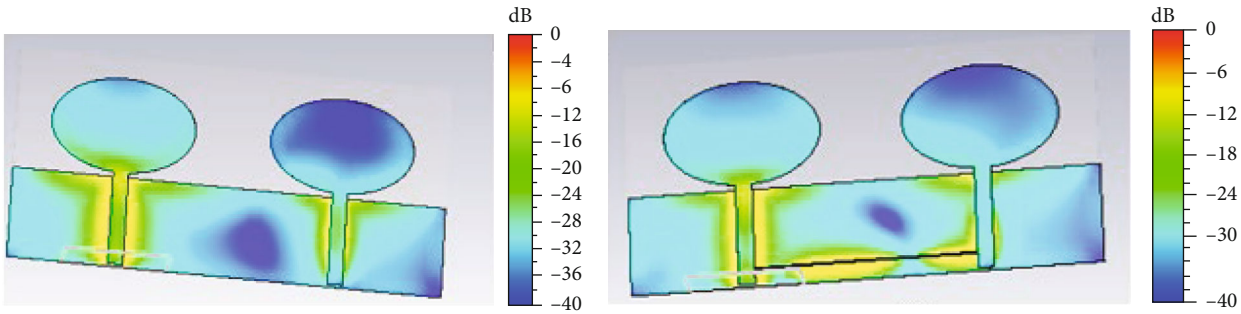

(a) (b)

Figure 14: Surface current distributions of multiantenna system at 3.5 GHz. (a) Without decoupling technique. (b) With neutralization decoupling technique.

carried out using a network analyzer (10 MHz-25 GHz). *S* -parameters simulation and measurement results of the proposed multiantenna configuration without decoupling technique are shown in Figure 19 below. As the two antennas are perfectly symmetrical, the *S*-parameters are also symmetrical. So, in Figure 19, we represent only the *S*-parameters of one antenna.

Taking into account the manufacturing accuracies, a good agreement between the simulations and the measured *S*-parameters can be obtained. On the other hand, comparing the simulations of this case with the case where each antenna is alone, we observe that each element resonated at 3.6 GHz with a reflexion coefficient S_{11} value of -46.87 dB. The transmission coefficient S_{21}, which is considered as the parameter characterizing the isolation between the two antenna feed ports, has a value of -11.66 dB at 3.5 GHz. This value of the mutual coupling between the antennas is estimated very high. This is due to the insufficient distance between each element, which results in a slight shift of 100 MHz of the resonant from 3.5 GHz to 3.6 GHz.

4.2.2. Fabricated Multi antennas Systems with Neutralization Decoupling Technique. We represent in Figure 20 below the realized prototype of the multiantenna system with neutralization. However, simulations and measurement results at 3.5 GHz of *S*-parameter are shown in Figure 21 below. As

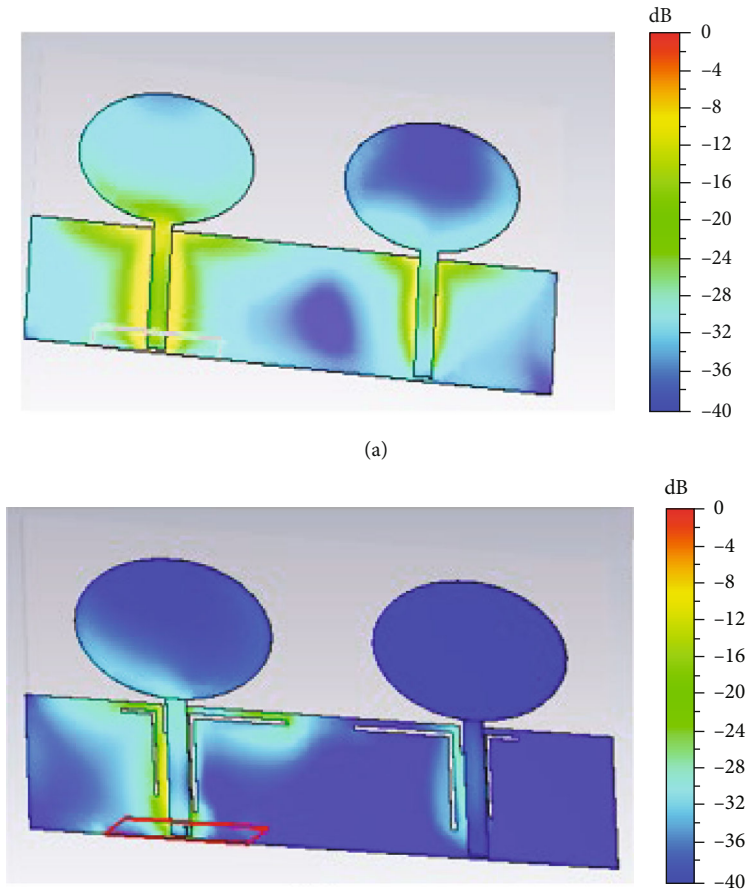

Figure 15: Surface current distributions of multiantenna system at 3.5 GHz. (a) Without decoupling technique. (b) With DGS decoupling technique.

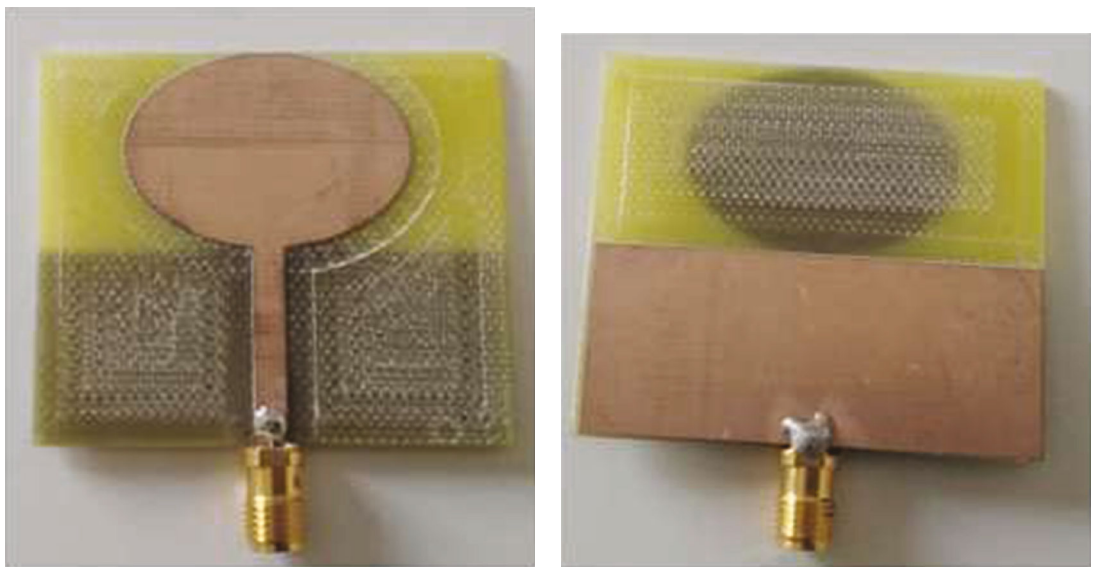

Figure 16: Realized prototype of the elliptical antenna element. (a) Top view. (b) Bottom view.

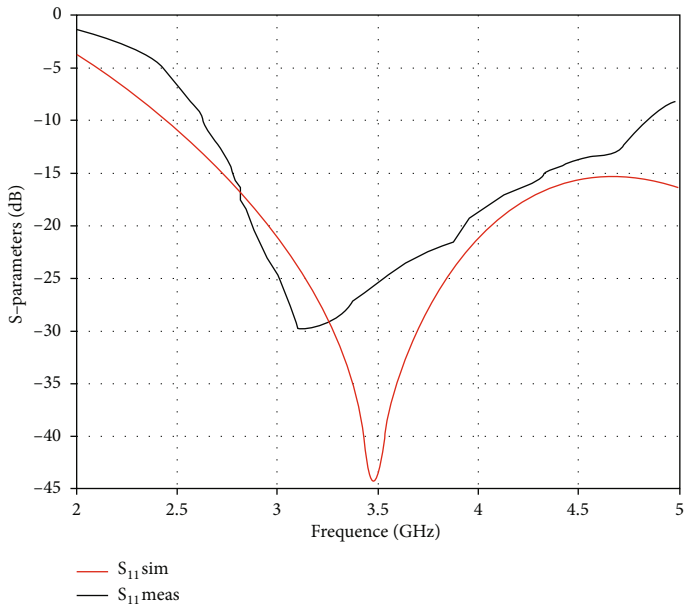

Figure 17: Simulated and measured reflection coefficient of the elliptical antenna as a function of frequency.

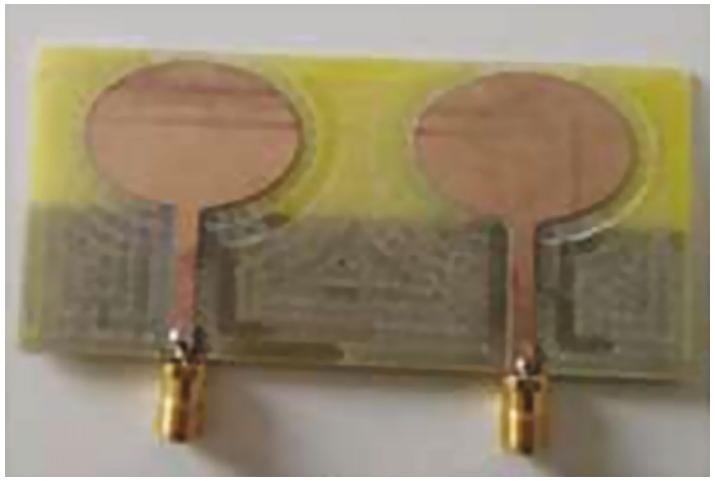

(a)

(b)

Figure 18: Realized prototypes of the antenna system. (a) Front view. (b) Bottom view.

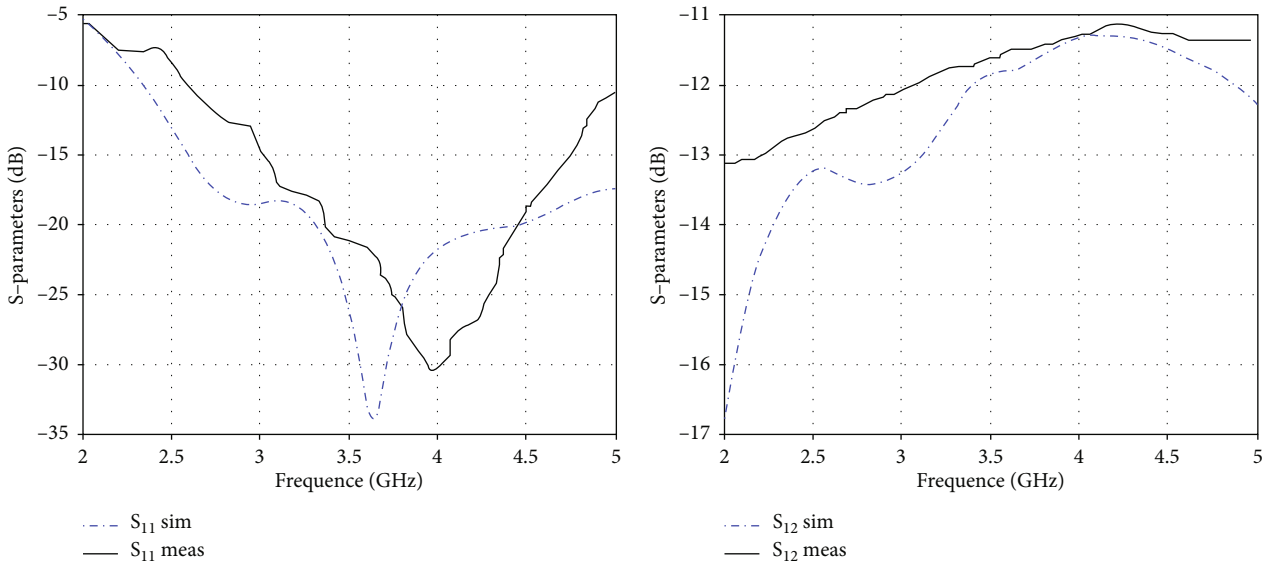

Figure 19: Simulated and measured *S*-parameters of elliptical multiantenna system without decoupling method (Antenna 1).

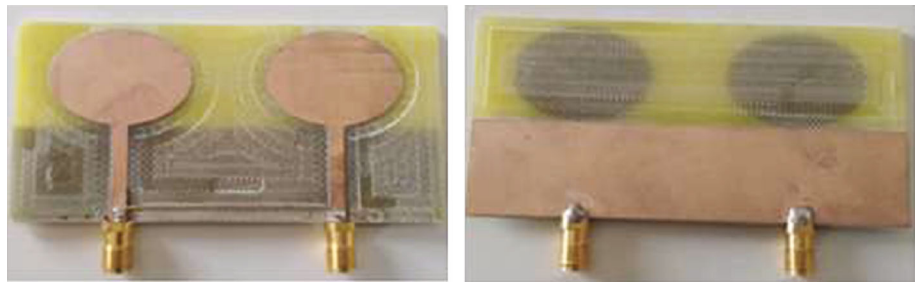

Figure 20: Realized prototype of the proposed multiantenna system with neutralization.

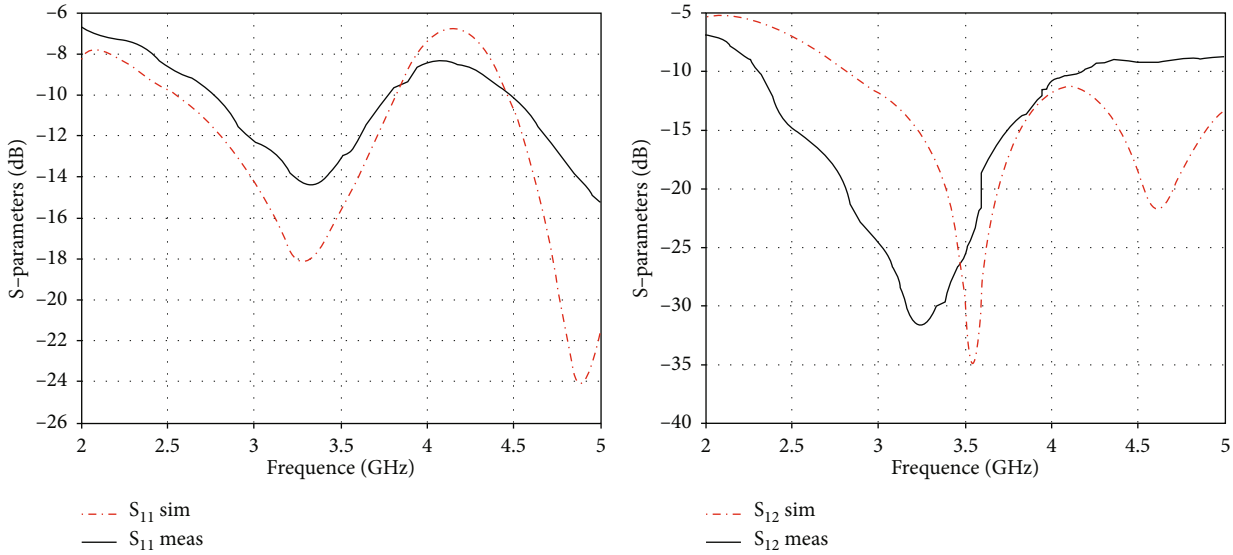

Figure 21: Simulated and measured *S*-parameters of the multiantenna system with neutralization (Antenna 1).

the two antennas are perfectly symmetrical, the *S*-parameters are also symmetrical. So, we represent only the *S*-parameters of one antenna. From these results, we noticed that the measurement results are close to the simulations, but 150 MHz shift of the resonance frequency is observed due to the manufacturing accuracies.

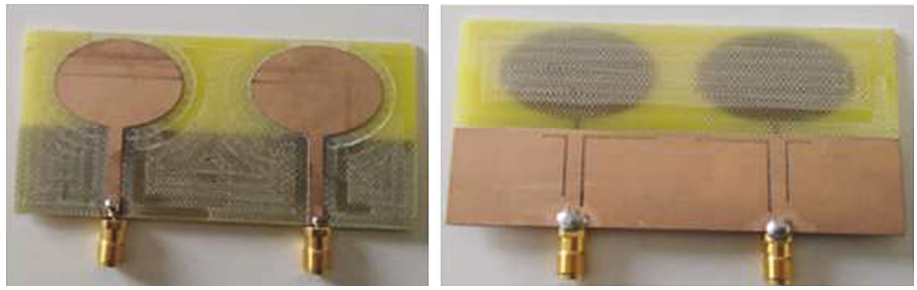

Figure 22: Realized prototype of the proposed multiantenna system with DGS.

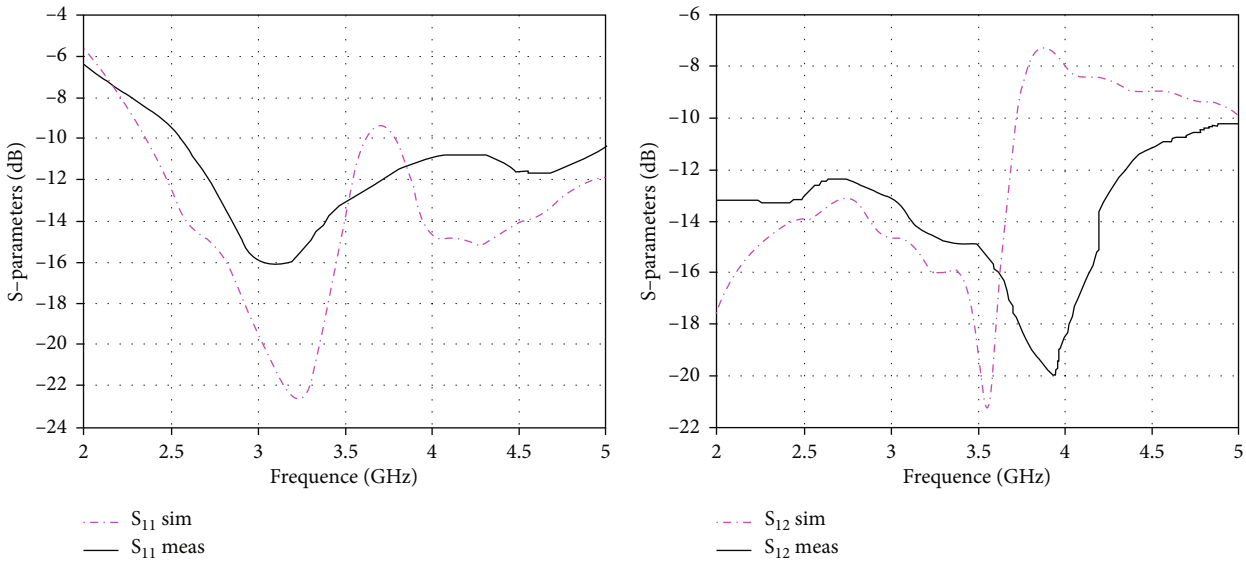

Figure 23: Simulated and measured *S*-parameters of the multiantenna system with DGS.

4.2.3. Fabricated Multi antennas Systems with DGS Decoupling Technique. We illustrate in Figure 22 the manufactured prototype of our proposed multi-antenna system with DGS decoupling technique, whereas in Figure 23, simulations and measurement results at 3.5 GHz of *S*-parameter (only of one antenna because of the symmetry of the structure) are presented. Analyzing Figure 23, we find that the measurement results are almost consistent with the simulations taking into account the accuracy of the manufacturing which generates a tolerable shift of 200 MHz of the resonance frequency.

4.3. Mimo Antenna Diversity Performances. The integration of several antennas on the same ground plan is a delicate challenge. In fact, there are some criteria of diversity performance is evaluated: the envelope correlation coefficient "ECC" which represents the main parameter, the diversity gain "DG" and the total efficiency. We present below these concerned parameters, simulated parameters processed with Matlab.

4.3.1. Envelope Correlation Coefficient (ECC). A multiantenna system with good diversity requires sufficient decorrelation of the signals received at its radiating elements [32]. This diversity performance can be characterized by the Envelope Correlation Coefficient (ECC) which describes the independence of the signals. So, using the correlation coefficient, we can understand the level of coupling that exists between the antenna ports in the MIMO system. This parameter is zero in the ideal case and should be less than 0.5 [33] in the case of a good diversity of antenna systems. A simplified approach lies in the calculation of the envelope correlation from the *S*-parameters of the antennas [34]. In this case, ECC for two-element antennas is calculated using *S*-parameters by the following equation:

$$\mathrm{ECC} = \frac{\left|S_{11}^{*}\,S_{12} + S_{21}^{*}\,S_{22}\right|^{2}}{\left(1 - \left(\left|S_{11}\right|^{2} + \left|S_{21}\right|^{2}\right)\right)\left(1 - \left(\left|S_{22}\right|^{2} + \left|S_{12}\right|^{2}\right)\right)}. \quad (1)$$

In the case of the curve presented in Figure 24 below, the ECC is calculated from the simulated *S*-parameters for multiantenna with neutralization and DGS. We notice that the obtained ECC level is always below 0.5 over the whole band [2–5] GHz for the two proposed multiantenna systems. Exactly at the study frequency of 3.5 GHz, ECC values are below 0.05 and 0.01, respectively, for neutralization and DGS multiantenna systems. This result is very satisfactory and shows that the signals have very good performances for the two proposed configurations.

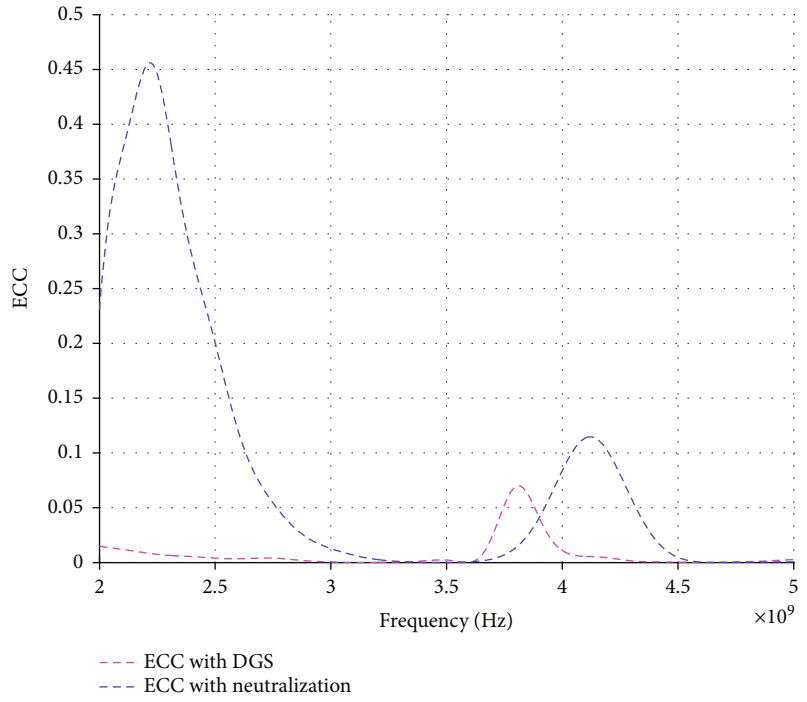

Figure 24: ECC simulated of multiantenna system with DGS and neutralization.

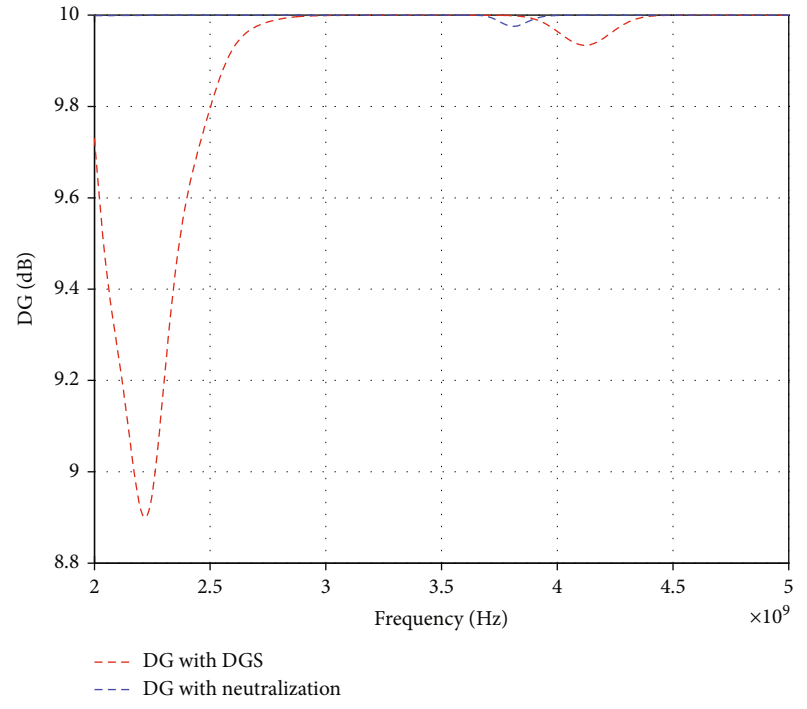

Figure 25: DG simulated of multiantenna system with DGS and neutralization.

4.3.2. Diversity Gain (DG). Diversity gain is a parameter that is defined to evaluate the benefit of using a diversity system [35]. It expresses the improvement in signal-to-noise ratio (SNR) of relative signals combined with respect to the SNR received on a single antenna. The diversity gain depends on a large part of the correlation envelope ECC, and it is calculated using the following formula:

$$\mathrm{DG} = 10.\sqrt{(1 - \mathrm{ECC})}. \quad (2)$$

Simulated DG for multiantenna system with neutralization and DGS is represented in Figure 25. We notice from this figure that the DG for the two configurations is around 10 dB and is at its maximum value exactly at the points

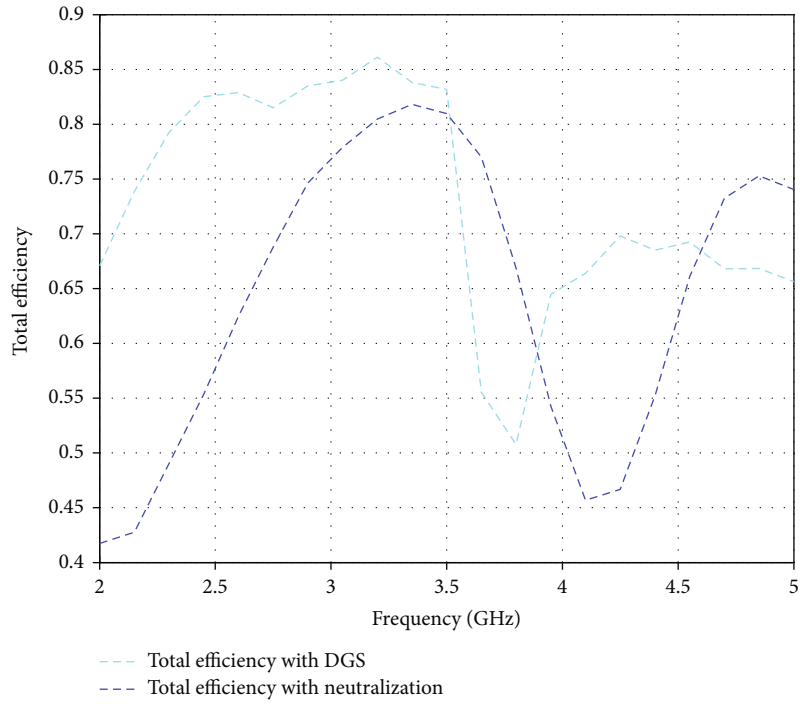

Figure 26: Total efficiency of multiantenna system with DGS and neutralization.

Table 2: Performance comparison of isolation techniques.

	Isolation with neutralization	Isolation with DGS
Couplage (dB)	-33 dB	-20 dB
Total efficiency	81%	83%
Envelope correlation coefficient (ECC)	<0.05	<0.01
Diversity gain (DG)	10 dB	10 dB

where the ECC is the lowest which is around the 3.5 GHz frequency.

4.3.3. Total Efficiency. In communication systems, the total efficiency of the antenna is the most important parameter, since it provides information on the performance of the wireless link. It is also valid for multiantenna and/or MIMO systems. This value can also be expressed with *S*-parameters and the radiated efficiency η_{rad} of the antenna as shown in the following equation [36]:

$$\eta_{\text{toti}} = \eta_{\text{rayi}} \left(1 - \sum_{n=1}^{N} \left| S_{n,1}{}^{2} \right| \right). \quad (3)$$

With "*i*", it is the antenna number "*i*" and *N* is the number on the antennas.

The total simulated efficiency for the two proposed configurations with neutralization and DGS is shown in Figure 26. These curves are plotted for only one antenna (port 1) due to the symmetry of the structures. A good total efficiency reaches 80% at 3.5 GHz for the two proposed multiantenna designs.

The performance of the two proposed 3.5 GHz isolation structures in terms of decoupling, total efficiency, ECC, and DG is summarized in Table 2 below. We can see that the two decoupling techniques proposed have very similar performances.

5. Conclusion

In this paper, we propose two multiantenna systems for 5G wireless applications with diversity. These systems consist of two elliptical antennas, respectively, with neutralization and DGS decoupling techniques. In fact, the insertion of a neutralization line between the two elements of a multiantenna system as well as the engraving of rectangular and L-shaped slots on the ground plan (DGS) of this system allows a reduction of mutual coupling and thus provides a better isolation between the elements that constitute it. Moreover, the use of these two isolations techniques provides diversity performance and guarantees an improvement of the overall radiation characteristics of the multiantenna system. This seems to be very interesting given the simplicity, low cost, little space occupied, and efficiency of the proposed solutions. This can be very suitable for 5G connected wireless applications devices.

Data Availability

The authors confirm that the data supporting the findings of this study are available within the article [and/or] its supplementary material.

Conflicts of Interest

The authors declare that they have no conflicts of interest.

References

[1] D. Wang, D. Chen, B. Song, N. Guizani, X. Yu, and X. du, "From IoT to 5G I-IoT: the next generation IoT-based intelligent algorithms and 5G technologies," *IEEE Communications Magazine*, vol. 56, no. 10, pp. 114–120, 2018.

[2] A. Ijaz, L. Zhang, M. Grau et al., "Enabling massive IoT in 5G and beyond systems: PHY radio frame design considerations," *IEEE Access*, vol. 4, pp. 3322–3339, 2016.

[3] W. Ejaz, A. Anpalagan, M. A. Imran et al., "Internet of Things (IoT) in 5G wireless communications," *IEEE Access*, vol. 4, pp. 10310–10314, 2016.

[4] W. Ejaz and M. Ibnkahla, "Multiband spectrum sensing and resource allocation for IoT in cognitive 5G networks," *IEEE Internet of Things Journal*, vol. 5, no. 1, pp. 150–163, 2018.

[5] A. C. Sodré, I. F. da Costa, R. A. dos Santos, H. R. D. Filgueiras, and D. H. Spadoti, "Waveguide-based antenna arrays for 5G networks," *International Journal of Antennas and Propagation*, vol. 2018, 10 pages, 2018.

[6] Q. Wang, N. Mu, L. L. Wang, S. Safavi-Naeini, and J. P. Liu, "5G MIMO conformal microstrip antenna design," *Wireless Communications and Mobile Computing*, vol. 2017, Article ID 7616825, 11 pages, 2017.

[7] H. al-Saif, M. Usman, M. T. Chughtai, and J. Nasir, "Compact ultra-wide band MIMO antenna system for lower 5G bands," *Wireless Communications and Mobile Computing*, vol. 2018, Article ID 2396873, 6 pages, 2018.

[8] A. Lapidoth and S. M. Moser, "Capacity bounds via duality with applications to multiple-antenna systems on flat-fading channels," *IEEE Transactions on Information Theory*, vol. 49, no. 10, pp. 2426–2467, 2003.

[9] M. Aldababsa, M. Toka, S. Gökçeli, G. K. Kurt, and O. Kucur, "A tutorial on nonorthogonal multiple access for 5G and beyond," *Wireless Communications and Mobile Computing*, vol. 2018, Article ID 9713450, 24 pages, 2018.

[10] L. Malviya, R. K. Panigrahi, and M. V. Kartikeyan, "MIMO antennas with diversity and mutual coupling reduction techniques: a review," *International Journal of Microwave and Wireless Technologies*, vol. 9, no. 8, pp. 1763–1780, 2017.

[11] I. Mohamed, M. Abdalla, and A. Mitkees, "Perfect isolation performance among two-element MIMO antennas," *AEU International Journal of Electronics and Communications*, vol. 107, pp. 21–31, 2019.

[12] W. Jiang, B. Liu, Y. Cui, and W. Hu, "High-isolation eight-element MIMO array for 5G smartphone applications," *IEEE Access*, vol. 7, pp. 34104–34112, 2019.

[13] Y. Li, C. Y. D. Sim, Y. Luo, and G. Yang, "High-isolation 3.5 GHz eight-antenna MIMO array using balanced open-slot antenna element for 5G smartphones," *IEEE Transactions on Antennas and Propagation*, vol. 67, no. 6, pp. 3820–3830, 2019.

[14] Y. Gao, *Characterisation of Multiple Antennas and Channel for Small Mobile Terminals, [Ph.D. thesis]*, University of London Queen Mary, 2007.

[15] Z. Li and Y. Rahmat-Samii, "Optimization of PIFA-IFA combination in handset antenna designs," *IEEE Transactions on Antennas and Propagation*, vol. 53, no. 5, pp. 1770–1778, 2005.

[16] Y. Tawk, K. Y. Kabalan, A. el-Hajj, C. G. Christodoulou, and J. Costantine, "A simple multiband printed bowtie antenna," *IEEE Antennas and Wireless Propagation Letters*, vol. 7, pp. 557–560, 2008.

[17] B. Lindmark and L. Garcia-Garcia, "Compact antenna array for MIMO applications at 1800 and 2450 MHz," *Microwave and Optical Technology Letters*, vol. 48, no. 10, pp. 2034–2037, 2006.

[18] M. I. Ahmed, A. Sebak, E. A. Abdallah, and H. Elhennawy, "Mutual coupling reduction using defected ground structure (DGS) for array applications," in *2012 15 International Symposium on Antenna Technology and Applied Electromagnetics*, pp. 1–5, Toulouse, France, 2012, IEEE.

[19] Jian Ren, Wei Hu, Yingzeng Yin, and Rong Fan, "Compact printed MIMO antenna for UWB applications," *IEEE Antennas and Wireless Propagation Letters*, vol. 13, pp. 1517–1520, 2014.

[20] D. Bhattacharya and M. Joshi, "DGS based mutual coupling reduction in an ultra-wide-band microstrip patch antenna array," in *2017 International Conference on Innovations in Information, Embedded and Communication Systems (ICIIECS)*, pp. 1–4, Coimbatore, India, 2017, IEEE.

[21] M. S. Teja and P. S. Rao, "Isolation enhancement of a very compact uwb-mimo slot antenna with two defected ground structures used in multi band applications," *International Research Journal of Engineering and Technology (IRJET)*, vol. 4, pp. 1967–1971, 2017.

[22] S. W. Su, C. T. Lee, and F. S. Chang, "Printed MIMO-antenna system using neutralization-line technique for wireless USB-dongle applications," *IEEE Transactions on Antennas and Propagation*, vol. 60, no. 2, pp. 456–463, 2012.

[23] S. Wang and Z. Du, "Decoupled dual-antenna system using crossed neutralization lines for LTE/WWAN smartphone applications," *IEEE Antennas and Wireless Propagation Letters*, vol. 14, pp. 523–526, 2015.

[24] J. H. Huang, W. J. Chang, and C. F. Jou, "Dual-band MIMO antenna with high isolation application by using neutralizing line," *Progress In Electromagnetics Research*, vol. 48, pp. 15–19, 2014.

[25] Y. S. Chen and H. C. Zhou, "An isolation-enhanced quad-element antenna using suspended solid wires for LTE small-cell base stations," *Radio Science*, vol. 52, no. 5, pp. 663–676, 2017.

[26] S. Zhang and G. F. Pedersen, "Mutual coupling reduction for UWB MIMO antennas with a wideband neutralization line," *IEEE Antennas and Wireless Propagation Letters*, vol. 15, pp. 166–169, 2015.

[27] P. Mondal, D. Dhara, and A. R. Harish, "A wideband slotted D-shaped monopole MIMO antenna with triple branch neutralization line," in *2018 IEEE Indian Conference on Antennas and Propogation (InCAP)*, pp. 1–4, Hyderabad, India, 2018, IEEE.

[28] I. Nadeem and D. Y. Choi, "Study on mutual coupling reduction technique for MIMO antennas," *IEEE Access*, vol. 7, pp. 563–586, 2019.

[29] A. R. Celik, M. B. Kurt, and S. Helhel, "Design of an elliptical planar monopole antenna for using in radar-based and ultra-wideband microwave imaging system," *International Research Journal of Engineering and Technology*, vol. 4, no. 11, pp. 1978–1983, 2017.

[30] M. N. Srifi and M. Essaaidi, *Ultra-wideband printed antennas design*, Ultra Wideband Communications: Novel Trends-Antennas and Propagation, 2011.

[31] A. Pingale, A. Shende, A. Jadhav, C. Ghanote, and U. Sonare, "Design of elliptical microstrip antenna for ultra wide band applications," *International Journal of Engineering and Technical Research (IJETR)*, vol. 3, no. 3, pp. 276–279, 2015.

[32] G. A. Mavridis, J. N. Sahalos, and M. T. Chryssomallis, "Spatial diversity two-branch antenna for wireless devices," *Electronics Letters*, vol. 42, no. 5, pp. 266–268, 2006.

[33] I. Salonen and P. Vainikainen, "Estimation of signal correlation in antenna arrays," *Proceedings JINA*, vol. 2, pp. 383–386, 2002.

[34] A. Diallo, C. Luxey, P. Lethuc, R. Staraj, and G. Kossiavas, "Enhanced diversity antennas for UMTS handsets," in *2006 First European Conference on Antennas and Propagation*, pp. 1–5, Nice, France, 2006, IEEE.

[35] A. Choumane, *Synthesis of a Propagation Channel by Multi-Antenna System for the Characterization of Mobile Terminals with Diversity, [Ph.D. thesis]*, Limoges, France, 2011.

[36] A. E. Ahmad, *Design of Array Antennas with Optimized Performance by Taking into Account Inter-Element Coupling: Application to Beamforming and Circular Polarization, [Ph.D. thesis]*, Limoges, France, 2010.